

Drag and lift

In Chapters 7 and 8 our study concerned 'internal flow' enclosed by solid walls. Now, how shall we consider such cases as the flight of a baseball or golf ball, the movement of an automobile or when an aircraft flies in the air, or where a submarine moves under the water? Here, flows outside such solid walls, i.e. 'external flows', are discussed.

9.1 Flows around a body

Generally speaking, flow around a body placed in a uniform flow develops a thin layer along the body surface with largely changing velocity, i.e. the boundary layer, due to the viscosity of the fluid. Furthermore, the flow separates behind the body, discharging a wake with eddies. Figure 9.1 shows the flows around a cylinder and a flat plate. The flow from an upstream point *a* is stopped at point *b* on the body surface with its velocity decreasing to zero; *b* is called a stagnation point. The flow divides into the upper and lower flows at point *b*. For a cylinder, the flow separates at point *c* producing a wake with eddies.

Let the pressure upstream at *a*, which is not affected by the body, be p_∞ , the flow velocity be U and the pressure at the stagnation point be p_0 . Then

$$p_0 = p_\infty + \frac{\rho U^2}{2} \quad (9.1)$$

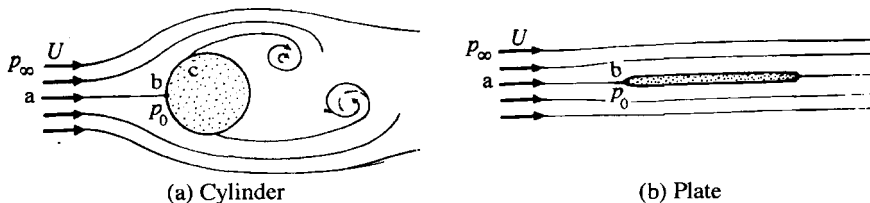


Fig. 9.1 Flow around a body

9.2 Forces acting on a body

Whenever a body is placed in a flow, the body is subject to a force from the surrounding fluid. When a flat plate is placed in the flow direction, it is only subject to a force in the downstream direction. A wing, however, is subject to the force R inclined to the flow as shown in Fig. 9.2. In general, the force R acting on a body is resolved into a component D in the flow direction U and the component L in a direction normal to U . The former is called drag and the latter lift.

Drag and lift develop in the following manner. In Fig. 9.3, let the pressure of fluid acting on a given minute area dA on the body surface be p , and the friction force per unit area be τ . The force $p dA$ due to the pressure p acts normal to dA , while the force due to the friction stress τ acts tangentially. The drag D_p , which is the integration over the whole body surface of the component in the direction of the flow velocity U of this force $p dA$, is called form drag or pressure drag. The drag D_f is the similar integration of τdA and is called the friction drag. D_p and D_f are shown as follows in the form of equations:

$$D_p = \int_A p dA \cos \theta \tag{9.2}$$

$$D_f = \int_A \tau dA \sin \theta \tag{9.3}$$

The drag D on a body is the sum of the pressure drag D_p and friction drag D_f , whose proportions vary with the shape of the body. Table 9.1 shows the contributions of D_p and D_f for various shapes. By integrating the component of $p dA$ and τdA normal to U , the lift L is obtained.

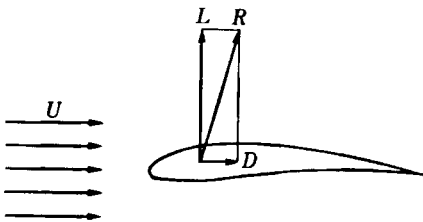


Fig. 9.2 Drag and lift

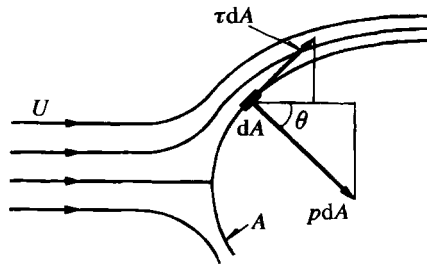


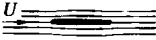



Fig. 9.3 Force acting on body

9.3 The drag of a body

9.3.1 Drag coefficient

The drag D of a body placed in the uniform flow U can be obtained from eqns (9.2) and (9.3). This theoretical computation, however, is generally difficult except for bodies of simple shape and for a limited range of velocity.

Table 9.1 Contributions of D_p and D_f for various shapes

Shape	Pressure drag D_p (%)	Friction drag D_f (%)
	0	100
	≈ 10	≈ 90
	≈ 90	≈ 10
	100	0

Therefore, there is no other way but to rely on experiments. In general, drag D is expressed as follows:

$$D = C_D A \frac{\rho U^2}{2} \quad (9.4)$$

where A is the projected area of the body on the plane vertical to the direction of the uniform flow and C_D is a non-dimensional number called the drag coefficient. Values of C_D for bodies of various shape are given in Table 9.2.

9.3.2 Drag for a cylinder

Ideal fluid

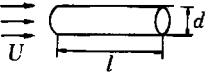
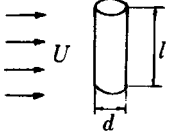
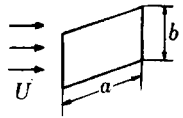

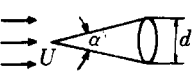


Let us theoretically study (neglecting the viscosity of fluid) a cylinder placed in a flow. The flow around a cylinder placed at right angles to the flow U of an ideal fluid is as shown in Fig. 9.4. The velocity v_θ at a given point on the cylinder surface is as follows (see Section 12.5.2):

$$v_\theta = 2U \sin \theta \quad (9.5)$$

Putting the pressure of the parallel flow as p_∞ , and the pressure at a given point on the cylinder surface as p , Bernoulli's equation produces the following result:

$$\begin{aligned} p_\infty + \frac{\rho U^2}{2} &= p + \frac{\rho v_\theta^2}{2} \\ p - p_\infty &= \frac{\rho(U^2 - v_\theta^2)}{2} = \frac{\rho U^2}{2}(1 - 4 \sin^2 \theta) \\ \frac{p - p_\infty}{\rho U^2/2} &= 1 - 4 \sin^2 \theta \end{aligned} \quad (9.6)$$

Table 9.2 Drag coefficients for various bodies

Body	Dimensional ratio	Datum area, A	Drag coefficient, C_D
Cylinder (flow direction) 	$l/d = 1$		0.91
	2		0.85
	4	$\frac{\pi}{4} d^2$	0.87
	7		0.99
Cylinder (right angles to flow) 	$l/d = 1$		0.63
	2		0.68
	5		0.74
	10	dl	0.82
	40		0.98
	∞		1.20
Oblong board (right angles to flow) 	$a/b = 1$		1.12
	2		1.15
	4		1.19
	10	ab	1.29
	18		1.40
	∞		2.01
Hemisphere (bottomless) 	I		0.34
	II	$\frac{\pi}{4} d^2$	1.33
Cone 	$a = 60^\circ$		0.51
	$a = 30^\circ$	$\frac{\pi}{4} d^2$	0.34
		$\frac{\pi}{4} d^2$	1.2
Ordinary passenger car 		Front projection area A	0.28–0.37

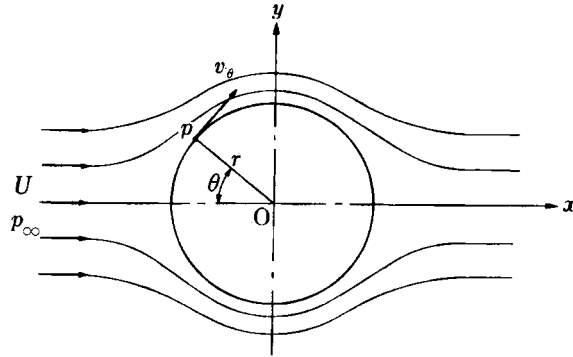


Fig. 9.4 Flow around a cylinder

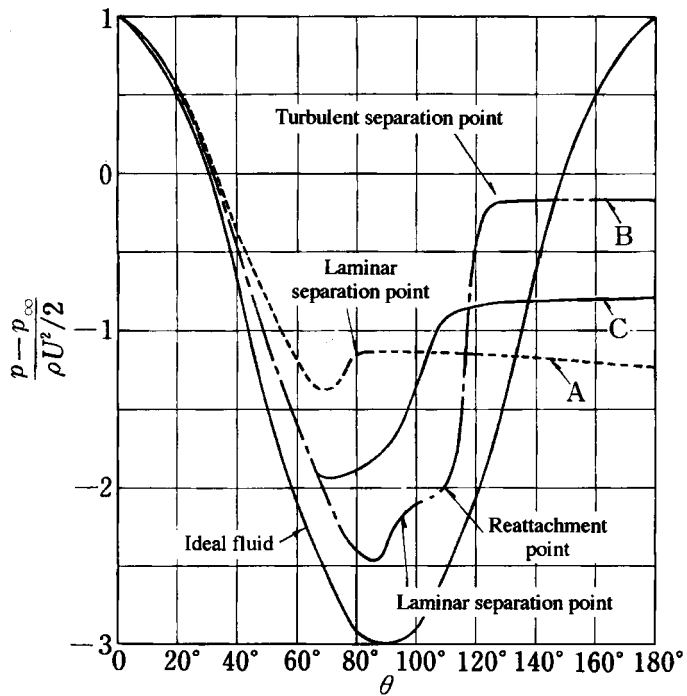


Fig. 9.5 Pressure distribution around cylinder: A, $Re = 1.1 \times 10^5 < Re_c$; B, $Re = 6.7 \times 10^5 > Re_c$; C, $Re = 8.4 \times 10^6 > Re_c$

This pressure distribution is illustrated in Fig. 9.5, where there is left and right symmetry to the centre line at right angles to the flow. Consequently the pressure resistance obtained by integrating this pressure distribution turns out to be zero, i.e. no force at all acts on the cylinder. Since this phenomenon is contrary to actual flow, it is called d'Alembert's paradox, after the French physicist (1717–83).

Viscous fluid

For a viscous flow, behind the cylinder, for very low values of $Re < 1$ ($Re = Ud/v$), the streamlines come together symmetrically as at the front of the cylinder, as indicated in Fig. 9.4. If Re is increased to the range $2 \sim 30$ the boundary layer separates symmetrically at position *a* (Fig. 9.6(a)) and two eddies are formed rotating in opposite directions.¹ Behind the eddies, the main streamlines come together. With an increase of Re , the eddies elongate and at $Re = 40 \sim 70$ a periodic oscillation of the wake is observed. These eddies are called twin vortices. When Re is over 90, eddies are continuously shed alternately from the two sides of the cylinder (Fig. 9.6(b)). Where $10^2 < Re < 10^5$, separation occurs near 80° from the front stagnation point (Fig. 9.6(c)). This arrangement of vortices is called a Kármán vortex street. Near $Re = 3.8 \times 10^5$, the boundary layer becomes turbulent and the separation position is moved further downstream to near 130° (Fig. 9.6(d)).

For a viscous fluid, as shown in Fig. 9.6, the flow lines along the cylinder surface separate from the cylinder to develop eddies behind it. This is visualised in Fig. 9.7. For the rear half of the cylinder, just like the case of a divergent pipe, the flow gradually decelerates with the velocity gradient reaching zero. This point is now the separation point, downstream of which flow reversals occur, developing eddies (see Section 7.4.2). This separation point shifts downstream as shown in Fig. 9.6(d) with increased $Re = Ud/v$ (d : cylinder diameter). The reason is that increased Re results in a turbulent boundary layer. Therefore, the fluid particles in and around the boundary layer mix with each other by the mixing action of the turbulent flow to make

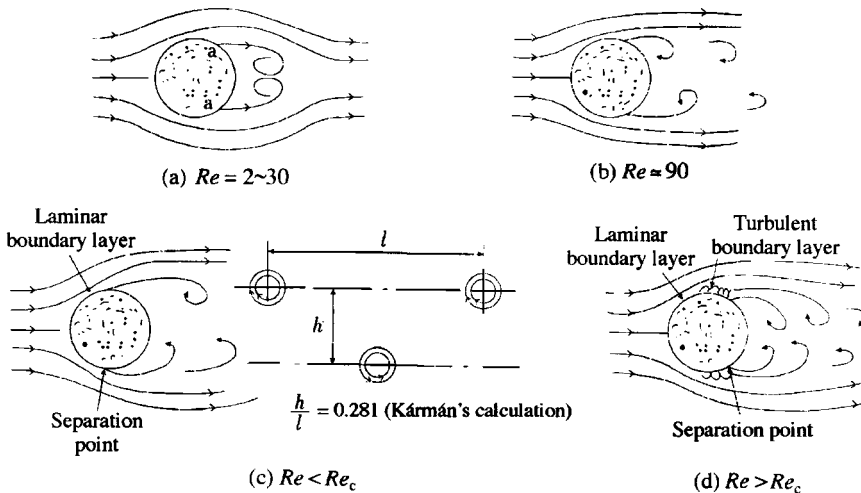


Fig. 9.6 Flow around a cylinder

¹ Streeter, V.L., *Handbook of Fluid Dynamics*, (1961), McGraw-Hill, New York.

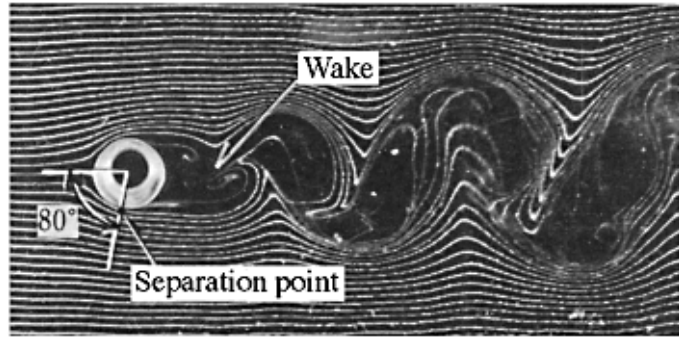


Fig. 9.7 Separation and Kármán vortex sheet (hydrogen bubble method) in water, velocity 2.4 cm/s, $Re = 195$

separation harder to occur. Figure 9.8 shows a flow visualisation of the development process from twin vortices to a Kármán vortex street. The Reynolds number $Re = 3.8 \times 10^5$ at which the boundary layer becomes turbulent is called the critical Reynolds number Re_c .

The pressure distribution on the cylinder surface in this case is like curves A, B and C in Fig. 9.5 with a reduced pressure behind the cylinder acting to produce a force in the downstream direction.

Figure 9.9 shows, for a cylinder of diameter d placed with its axis normal to a uniform flow U , changes in drag coefficient C_D with Re and also

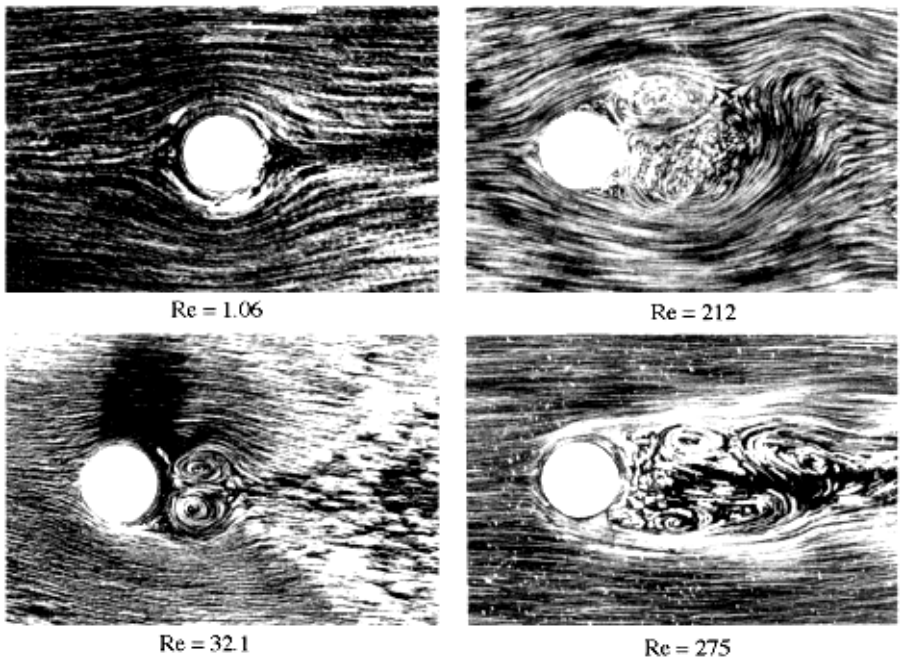


Fig. 9.8 Flow around a cylinder

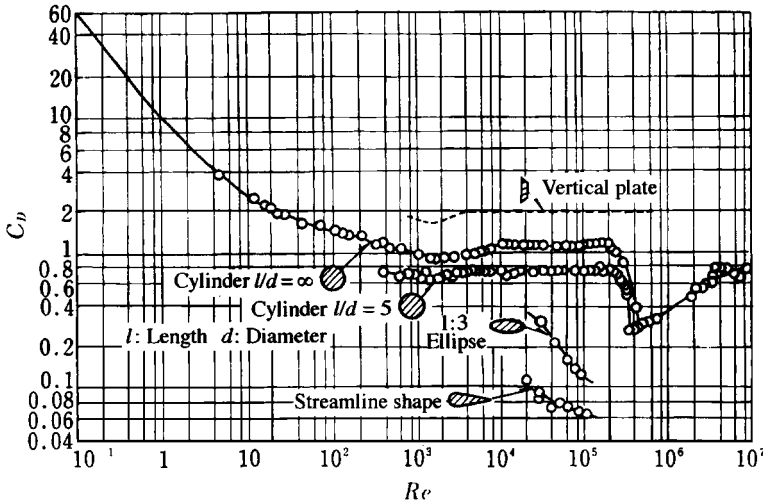


Fig. 9.9 Drag coefficients for cylinders and other column-shaped bodies

comparison with oblong and streamlined columns.² When $Re = 10^3 \sim 2 \times 10^5$, $C_D = 1 \sim 1.2$ or a roughly constant value; but when $Re = 3.8 \times 10^5$ or so, C_D suddenly decreases to 0.3. To explain this phenomenon, it is surmised that the location of the separation point suddenly changes as it reaches this Re , as shown in Fig 9.6(d).

G. I. Taylor (1886–1975, scholar of fluid dynamics at Cambridge University) calculated the number of vortices separating from the body every second, i.e. developing frequency f for $250 < Re < 2 \times 10^5$, by the following equation:

$$f = 0.198 \frac{U}{d} \left(1 - \frac{19.7}{Re} \right) \tag{9.7}$$

fd/U is a dimensionless parameter called the Strouhal number St (named after V. Strouhal (1850-1922), a Czech physicist; in 1878, he first investigated the ‘singing’ of wires), which can be used to indicate the degree of regularity in a cyclically fluctuating flow.

When the Kármán vortices develop, the body is acted on by a cyclic force and, as a result, it sometimes vibrates to produce sounds. The phenomenon where a power line ‘sings’ in the wind is an example of this.

In general, most drag is produced because a stream separates behind a body, develops vortices and lowers its pressure. Therefore, in order to reduce the drag, it suffices to make the body into a shape from which the flow does not separate. This is the so-called streamline shape.

² Hoerner, S.F., *Fluid Dynamic Drag*, (1965), Hoerner, Midland Park, NJ.

9.3.3 Drag of a sphere

The drag coefficient of a sphere changes as shown in Fig. 9.10.³ Within the range where Re is fairly high, $Re = 10^3 \sim 2 \times 10^5$, the resistance is proportional to the square of the velocity, and C_D is approximately 0.44. As Re reaches 3×10^5 or so, like the case of a cylinder the boundary layer changes from laminar flow separation to turbulent flow separation. Therefore, C_D decreases to 0.1 or less. On reaching higher Re , C_D gradually approaches 0.2.

Slow flow around a sphere is known as Stokes flow. From the Navier-Stokes equation and the continuity equation the drag D is as follows:

$$\left. \begin{aligned} D &= 3\pi\mu U d \\ C_D &= \frac{24}{Re} \end{aligned} \right\} \quad (9.8)$$

This is known as Stokes' equation.⁴ This coincides well with experiments within the range of $Re < 1$.

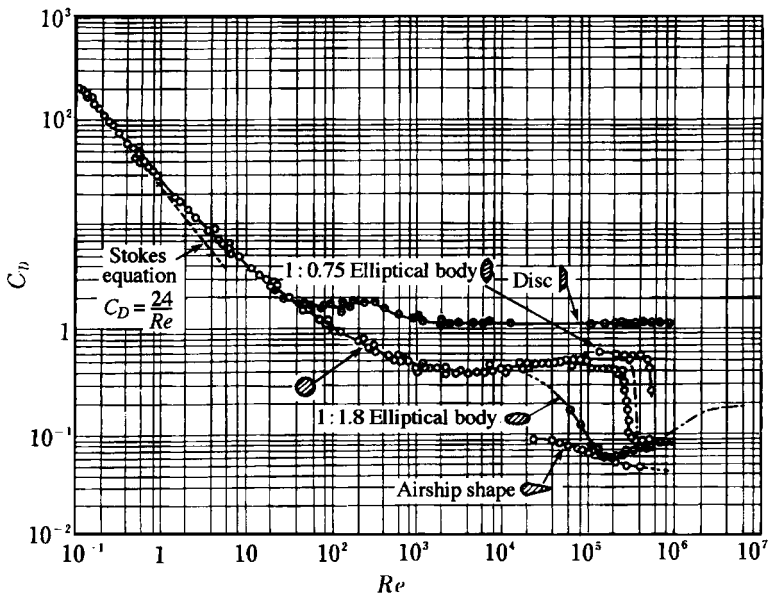


Fig. 9.10 Drag coefficients of a sphere and other three-dimensional bodies

9.3.4 Drag of a flat plate

As shown in Fig. 9.11, as a uniform flow of velocity U flows parallel to a flat plate of length l , the boundary layer steadily develops owing to viscosity.

³ Streeter, V.L., *Handbook of Fluid Dynamics*, (1961), McGraw-Hill, New York.

⁴ Lamb, H., *Hydrodynamics*, 6th edition, (1932), Cambridge University Press.

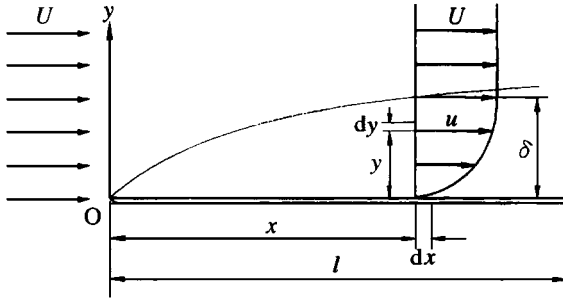


Fig. 9.11 Flow around a flat plate

Now, set the thickness of the boundary layer at a distance x from the leading edge of the flat plate to δ . Consider the mass flow rate of the fluid $\rho u dy$ flowing in the layer dy within the boundary layer at the given point x . From the difference in momentum of this flow quantity $\rho u dy$ before and after passing over this plate, the drag D due to the friction on the plate is as follows:

$$D = \int_0^\delta \rho u(U - u)dy \tag{9.9}$$

Now, putting the wall face friction stress as τ_0 , and since $dD = \tau_0 dx$, then from above

$$\tau_0 = \frac{dD}{dx} = \rho \frac{d}{dx} \int_0^\delta u(U - u)dy \tag{9.10}$$

Laminar boundary layer

Now, treating the distribution of u as a parabolic velocity distribution like the laminar flow in a circular pipe,

$$\eta = \frac{y}{\delta} \quad \frac{u}{U} = 2\eta - \eta^2 \tag{9.11}$$

Substituting the above into eqn (9.10),

$$\tau_0 = \rho U^2 \frac{d\delta}{dx} \int_0^1 \frac{u}{U} \left(1 - \frac{u}{U}\right) d\eta = 0.133 \rho U^2 \frac{d\delta}{dx} \tag{9.12}$$

On the other hand,

$$\tau_0 = \mu \left. \frac{du}{dy} \right|_{y=0} = 2 \frac{\mu U}{\delta} \tag{9.13}$$

Therefore, from eqns (9.12) and (9.13),

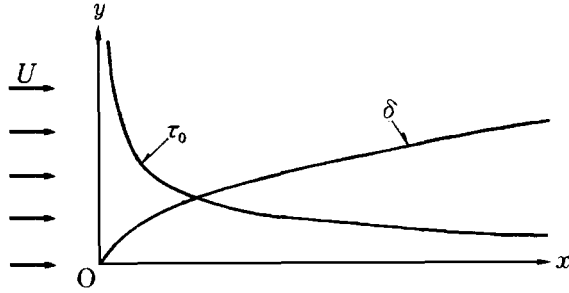


Fig. 9.12 Changes in boundary layer thickness and friction stress along a flat plate

$$\delta d\delta = 15.04 \frac{\mu}{\rho U} dx$$

$$\frac{\delta^2}{2} 15.04 \frac{\nu}{U} x + c$$

From $x = 0$ and $\delta = 0$, $c = 0$. Therefore

$$\delta = 5.48 \sqrt{\frac{\nu x}{U}} = \frac{5.48}{\sqrt{R_x}} x \quad (9.14)$$

However, since $R = U_x/\nu$, substitute eqn (9.14) into (9.13),

$$\tau_0 = 0.365 \sqrt{\frac{\mu \rho U^3}{x}} = 0.730 \frac{\rho U^2}{2} \sqrt{\frac{\nu}{U x}} \quad (9.15)$$

As shown in Fig. 9.12, the boundary layer thickness δ increases in proportion to \sqrt{x} , while the surface frictional stress reduces in inverse proportion to \sqrt{x} .

The friction resistance for width b of the whole (but one face only) of that plate is expressed as follows by integrating eqn (9.15):

$$D = \int_0^l \tau_0 dx = 0.73 \sqrt{\mu \rho U^3} l b \quad (9.16)$$

$$D = C_f l \frac{\rho U^2}{2} \quad (9.17)$$

Defining the friction drag coefficient as C_f , this becomes

$$C_f = \frac{1.46}{\sqrt{R_l}} \quad (9.18)$$

where $R = Ul/\nu$. The above equations roughly coincide with experimental values within the range of $R < 5 \times 10^5$.

Turbulent boundary layer

Whenever R_l is large, the length of laminar boundary layer is so short that the layer can be regarded as a turbulent boundary layer over the full length of a flat plate. Now, assume the distribution of u to be given by

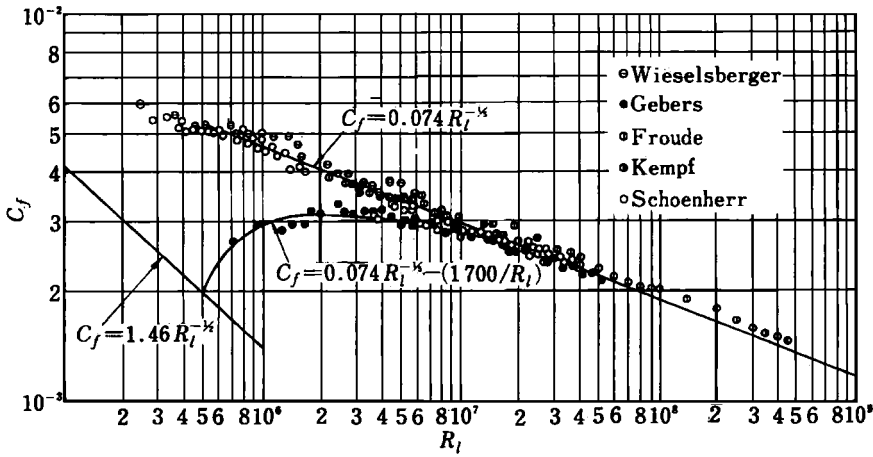


Fig. 9.13 Friction drag coefficients of a flat plate

$$\frac{u}{U} = \left(\frac{y}{\delta}\right)^{1/7} = \eta^{1/7} \tag{9.19}$$

like turbulent flow in a circular pipe, and the following equations are obtained:⁵

$$\delta = \frac{0.37x}{R_x^{1/5}} \tag{9.20}$$

$$\tau_0 = 0.029\rho U^2 \left(\frac{\nu}{Ux}\right)^{1/5} \tag{9.21}$$

$$D = \frac{0.036\rho U^2 l}{R_l^{1/5}} \tag{9.22}$$

$$C_f = 0.072R_l^{-1/5} \tag{9.23}$$

The above equations coincide well with experimental values within the range of $5 \times 10^5 < R_l < 10^7$. From experimental data,

$$C_f = 0.074R_l^{-1/5} \tag{9.24}$$

gives better agreement.

In the case where there is a significant length of laminar boundary layer at the front end of a flat plate, but later developing into a turbulent boundary layer, eqn (9.12) is amended as follows:

$$C_f = \frac{0.074}{R_l^{1/5}} - \frac{1700}{R_l} \tag{9.25}$$

The relationship of C_f with R_l is shown in Fig. 9.13.

⁵ Streeter, V. L., *Handbook of Fluid Dynamics*, (1961), McGraw-Hill, New York.

9.3.5 Friction torque acting on a revolving disc

If a disc revolves in a fluid at angular velocity ω , a boundary layer develops around the disc owing to the fluid viscosity.

Now, as shown in Fig. 9.14, let the radius of the disc be r_0 , the thickness be b , and the resistance acting on the elementary ring area $2\pi r dr$ at a given radius $r\omega$ be dF . Assuming that dF is proportional to the square of the circular velocity $r\omega$ of that section, and the friction coefficient is f , the torque T_1 due to this surface friction is as follows:

$$dF = f \frac{\rho(r\omega)^2}{2} 2\pi r dr$$

or

$$T_1 = \int_{r=0}^{r_0} r dF = \frac{\pi f}{5} \rho \omega^2 r_0^5 \quad (9.26)$$

Now, putting the friction coefficient at the cylindrical part of the disc to f' and the resistance acting on it to F' ,

$$F' = f' \frac{\rho(r_0\omega)^2}{2} 2\pi r_0 b$$

Torque T_2 due to this surface friction is as follows:

$$T_2 = \pi f' \rho \omega^2 r_0^4 b \quad (9.27)$$

Assuming $f = f'$, the torque T needed for rotating this disc is

$$T = 2T_1 + T_2 = \pi f \rho \omega^2 r_0^4 \left(\frac{2}{5} r_0 + b \right) \quad (9.28)$$

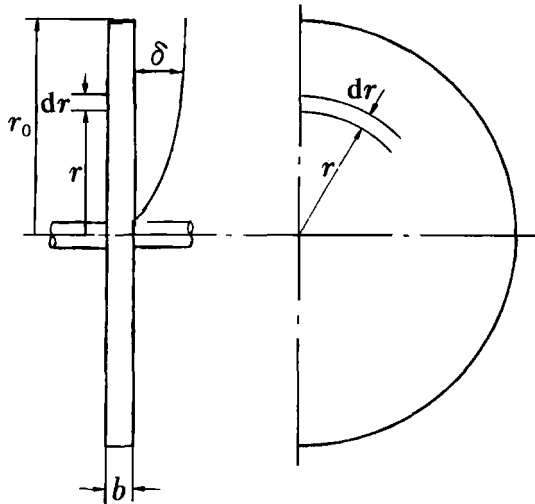


Fig. 9.14 A revolving disc

and the power L needed in that case is

$$L = T\omega = \pi f \rho \omega^3 r_0^4 \left(\frac{2}{5} r_0 + b \right) \quad (9.29)$$

These relationships are used for such cases as computing the power loss due to the friction of the impeller of a centrifugal pump or water turbine.

9.4 The lift of a body

9.4.1 Development of lift

Consider a case where, as shown in Fig. 9.15, a cylinder placed in a uniform flow U rotates at angular velocity ω but without flow separation. Since the fluid on the cylinder surface moves at a circular velocity $u = r_0\omega$, sticking to the cylinder owing to the viscosity of the fluid, the flow velocity at a given point on the cylinder surface (angle θ) is the tangential velocity v_θ caused by the uniform flow U plus u . In other words, $2U \sin \theta + r_0\omega$.

Putting the pressure of the uniform flow as p_∞ , and the pressure at a given point on the cylinder surface as p , while neglecting the energy loss because it is too small, then from Bernoulli's equation

$$p_\infty + \frac{\rho}{2} U^2 = p + \frac{\rho}{2} (2U \sin \theta + r_0\omega)^2$$

Therefore

$$\frac{p - p_\infty}{\rho U^2 / 2} = 1 - \left(\frac{2U \sin \theta + r_0\omega}{U} \right)^2 \quad (9.30)$$

Consequently, for unit width of the cylinder surface, integrate the component in the y direction of the force due to the pressure $p - p_\infty$ acting on a minute area $r_0 d\theta$, and the lift L acting on the unit width of cylinder is obtained:

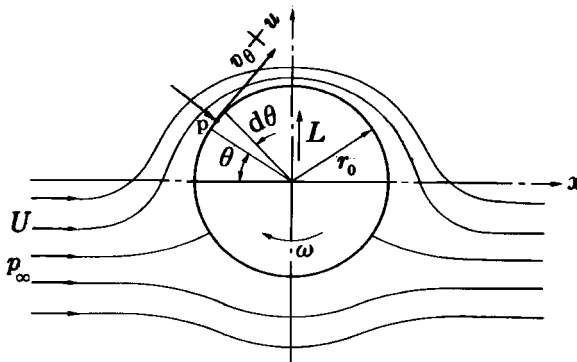


Fig. 9.15 Lift acting on a rotating cylinder

$$\begin{aligned}
L &= 2 \int_{-\pi/2}^{\pi/2} -(p - p_{\infty})r_0 \, d\theta \sin \theta \\
&= -r_0 \rho U^2 \int_{-\pi/2}^{\pi/2} \left[1 - \left(\frac{2U \sin \theta + r_0 \omega}{U} \right)^2 \right] \sin \theta \, d\theta \\
&= -r_0 \rho U^2 \int_{-\pi/2}^{\pi/2} \left[1 - \left(\frac{r_0 \omega}{U} \right)^2 - \frac{4r_0 \omega}{U} \sin \theta - 4 \sin^2 \theta \right] \sin \theta \, d\theta \\
&= 2\pi r_0^2 \omega \rho U = 2\pi r_0 u \rho U \tag{9.31}
\end{aligned}$$

The circulation around the cylinder surface when a cylinder placed in a uniform flow U has circular velocity u is

$$\Gamma = 2\pi r_0 u$$

Substituting the above into eqn (9.31),

$$L = \rho U \Gamma \tag{9.32}$$

This lift is the reason why a baseball, tennis ball or golf ball curves or slices if spinning.⁶ This equation is called the Kutta–Joukowski equation.

In general, whenever circulation develops owing to the shape of a body placed in the uniform flow U (e.g. aircraft wings or yacht sails) (see Section 9.4.2), lift L as in eqn (9.32) is likewise produced for the unit width of its section.

9.4.2 Wing

Of the forces acting on a body placed in a flow, if the body is so manufactured as to make the lift larger than the drag, it is called a wing, aerofoil or blade.

The shape of a wing section is called an aerofoil section, an example of which is shown in Fig. 9.16. The line connecting the leading edge with the trailing edge is called the chord, and its length is called the chord length. The line connecting the mid-points of the upper and lower faces of the aerofoil



⁶ The reason why the golf ball surface has many dimple-like hollows is to reduce the air resistance by producing turbulence around the ball, and to produce an effective lift while keeping a stable flight by making the air circulation larger (see Plate 4). The number of rotations (called spin) per second of a golf ball can be 100 or more.

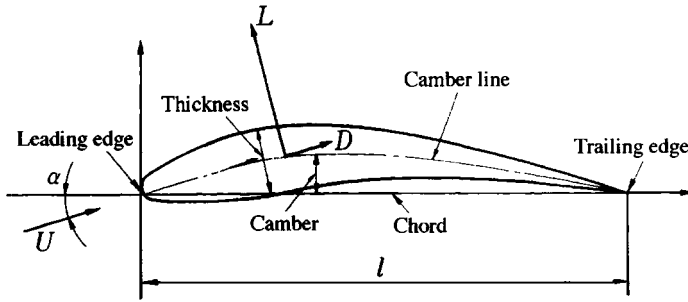


Fig. 9.16 An aerofoil section

section is called the camber line. The height of the camber line from the chord is called the camber, which mostly means its maximum value in particular. The thickness of a wing as measured vertically to the camber or chord is called its thickness, whose maximum value is called the maximum thickness. Furthermore, the angle α between the chord and the flow direction U is called the angle of attack. Putting the wing width as b , and the maximum projection area of the wing as A , b^2/A is called the aspect ratio. Assuming the length of the chord is l , since $A = bl$ for an oblong wing, the aspect ratio becomes $b^2/A = b/l$.

Of the studies on the characteristics of wing shape, those most well known have been performed by the USA's NACA (National Advisory Committee for Aeronautics, renamed in 1959 as NASA (National Aeronautics and Space Administration)), by the UK's RAE (Royal Aircraft Establishment) and by Germany's Göttingen University. The particular wing shapes are named after them.

The lift L , drag D and moment M (moment about the wing leading edge or the point on the chord $l/4$ from the leading edge) acting on the wing are expressed respectively for unit width by the following equations:

$$\left. \begin{aligned} L &= C_L l \frac{\rho U^2}{2} \\ D &= C_D l \frac{\rho U^2}{2} \\ M &= C_M l^2 \frac{\rho U^2}{2} \end{aligned} \right\} \quad (9.33)$$

C_L , C_D and C_M are called respectively the lift coefficient, drag coefficient and moment coefficient to be determined by the aerofoil section, Mach number and Reynolds number. The wing characteristic is indicated by the values of C_L , C_D and C_M for the angle of attack α , or by plotting C_D and C_M on the abscissa and C_L on the ordinate. These plots are called the characteristic curves. Some examples of them are shown in Figs 9.17, 9.19 and 9.20.

The lift coefficient C_L reaches zero at a certain angle of attack α , called the zero lift angle. As the angle of attack increases from the zero lift angle,

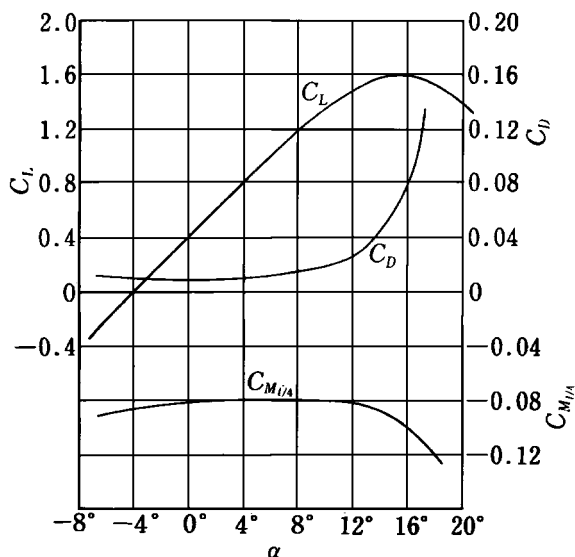


Fig. 9.17 Characteristic curves of a wing

the lift coefficient C_L increases in a straight line. As it further increases, however, the increase in C_L gradually slows down, reaches a maximum value at a certain point, and thereafter suddenly decreases. This is due to the fact that, as shown in Fig. 9.18, the flow separates on the upper surface of the wing because the angle of attack has increased too much. This phenomenon is completely analogous to the separation occurring on a divergent pipe or flow behind a body and is called stall. Angle α at which C_L reaches a maximum is the stalling angle and the maximum value of C_L is the maximum lift coefficient. Figure 9.19 shows the characteristic with changing wing section.

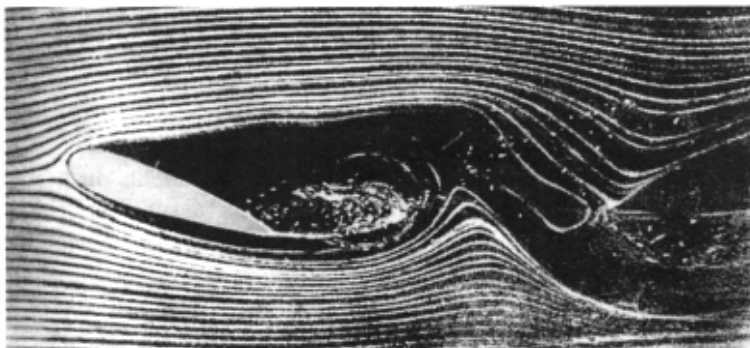


Fig. 9.18 Flow around a stalled wing

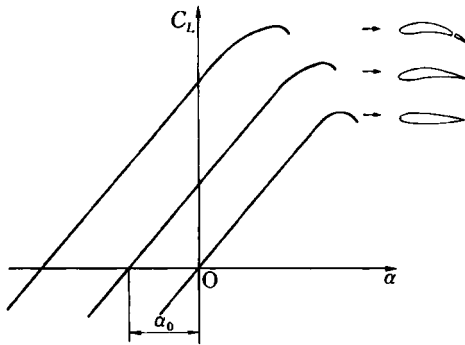


Fig. 9.19 Aerofoil section and characteristic

Figure 9.20 shows a wing characteristic by putting C_D on the abscissa and C_L on the ordinate, and is called the lift-drag polar, from which the angle of attack maximising the lift-drag ratio C_L/C_D can easily be found.

The reason why a wing produces lift is because a circulatory flow is produced just like for a rotating cylinder. In the case of a wing section, the circulatory flow is produced because the trailing edge is sharpened. A wing moves from a stationary state initially as shown in Fig. 9.21(a). Owing to its behaviour as potential flow, a rear stagnation point develops at point A. Consequently, the flow develops into a flow running round the trailing edge B. Since the trailing edge is sharp, however, the flow is unable to run round the wing surface but separates from it producing a vortex as shown in (b) of

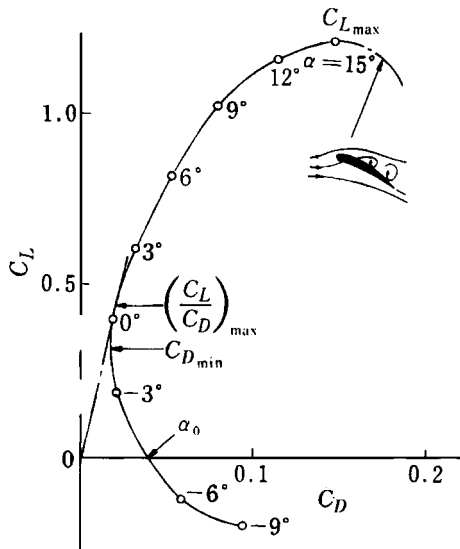


Fig. 9.20 Characteristic curve of a wing (lift-drag curve)

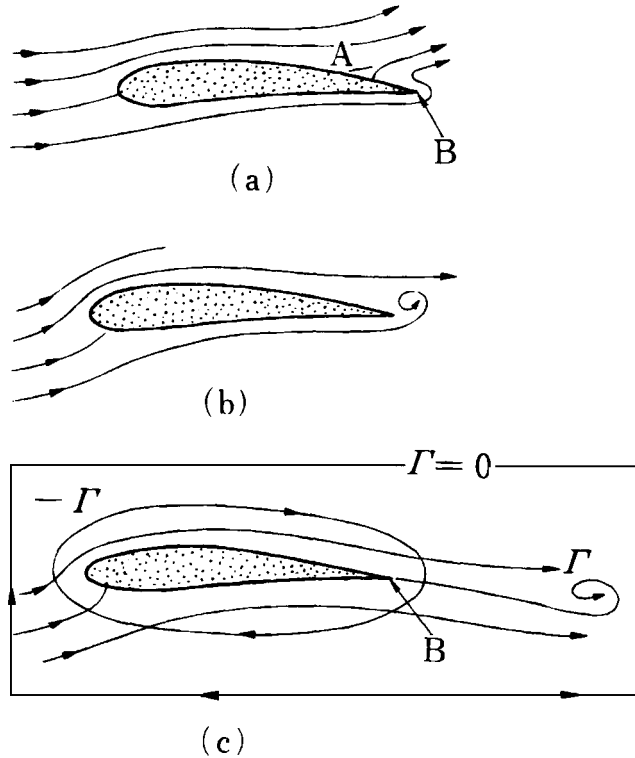


Fig. 9.21 Development of circulation around aerofoil section

the same figure. This vortex moves backwards being driven by the main flow. The flow on the upper surface of the wing is drawn towards the trailing edge, which itself develops into a stagnation point, and thus the flow is now as shown in (c) of the same figure. As one vortex is produced, another vortex of equal strength is also produced since the flow system as a whole should be in a net non-rotary movement. Therefore a circulation is produced against the start-up vortex as if another vortex of equal strength in counterrotation had developed around the wing section. The former vortex is called a starting-up vortex because it is left at the starting point; the latter assumed vortex is a wing-bound vortex. The situation where the flow runs off the sharp trailing edge of a wing as stated above is called the Kutta condition or Joukowski's hypothesis. Figure 9.22 shows the visualised picture of a starting vortex.

The blades of a blower, compressor, water wheel, steam turbine or gas turbine of the axial flow type are distributed radially in planes around the shaft and the blade sections of the same shape are found arranged at a certain spacing as shown in Fig. 9.23. This is called a cascade.

The action of a cascade is to change the flow direction with small loss by using the necessary stagger angle.

The lift acting on a blade is expressed by $\rho v_{\infty} \Gamma$ from eqn (9.32) where v_{∞}

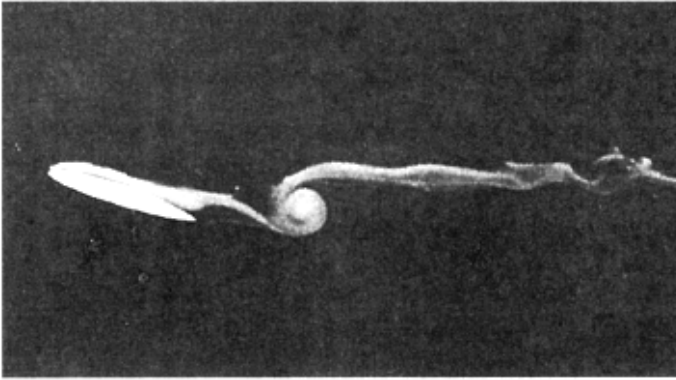


Fig. 9.22 Starting vortex (courtesy of the National Physical Laboratory)

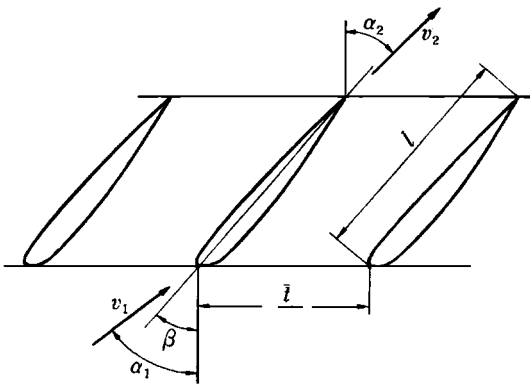


Fig. 9.23 Cascade: v_1 , v_2 , velocities at infinity in front and behind the cascade; α_1 , inlet angle (angle of velocity v_1 to axial direction); α_2 , exit angle (angle of velocity v_2 to axial direction); l , chord length; t , space between blades; l/t , solidity; β , stagger angle; $\theta = \alpha_1 - \alpha_2$, turning angle of flow

represents the mean flow velocity of v_1 and v_2 . The magnitude of the circulation around a blade in a cascade is affected by the other blades giving less lift compared with a solitary blade.

For the same blade section, setting the lifts of a solitary blade and a cascade blade to L_0 and L respectively,

$$k = L/L_0 \quad (9.34)$$

k is called the interference coefficient. It is a function of l/t and β , and is near one whenever l/t is 0.5 or less.

9.5 Cavitation

According to Bernoulli's principle, as the velocity increases, the pressure decreases correspondingly. In the forward part on the upper surface of a wing

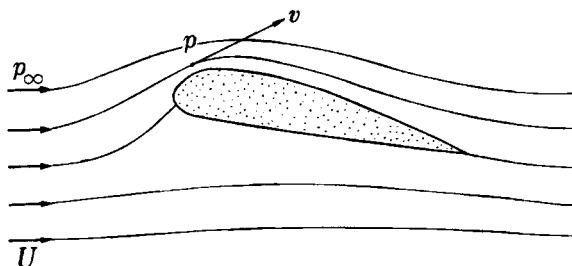


Fig. 9.24 An aerofoil section inside the flow

section placed in a uniform flow as shown in Fig. 9.24, for example, the flow velocity increases while the pressure decreases.

If a section of a body placed in liquid increases its velocity so much that the pressure there is less than the saturation pressure of the liquid, the liquid instantaneously boils, producing bubbles with cavities. This phenomenon is called cavitation. In addition, since gas dissolves in liquid in proportion to the pressure (Henry's Law), as the liquid pressure decreases, the dissolved gas separates from the liquid into bubbles even before the saturation pressure is reached. When these bubbles are conveyed downstream where the pressure is higher they are suddenly squeezed and abnormally high pressure develops.⁷ At this point noise and vibration occur eroding the neighbouring surface and leaving on it holes small in diameter but relatively deep, as if made by a slender drill in most cases. These phenomena as a whole are also referred to as cavitation in a wider sense.

The blades of a pump or water wheel, or the propeller of a boat, are sometimes destroyed by such phenomena. They can develop on liquid-carrying pipe lines or on hydraulic devices and cause failures.

The saturation pressures at various temperatures are shown in Table 9.3, while the volume ratios of air soluble in water at 1 atm are given in Table 9.4.

When an aerofoil section is placed in a flow of liquid, the pressure distribution on its surface is as shown in Fig. 9.25. As the cavity grows, the upper pressure characteristic curve lowers while vibration etc. grow. When the liquid pressure is low and the flow velocity is large, the cavity grows further. When it grows beyond twice the chord length, the flow stabilises, with noise and vibration reducing. This situation is called supercavitation, and is applied to the wings of a hydrofoil boat.

Let the upstream pressure not affected by the wing be p_∞ , the flow velocity U and the saturation pressure p_v . When the pressure at a point on the wing surface or nearby has reached p_v , cavitation develops. The ratio of $p_\infty - p_v$ to the dynamic pressure is expressed by the following equation:

⁷ According to actual measurements, a pressure of 100–200 atmospheres, or sometimes as high as 500 atmospheres, is brought about.

Table 9.3 Saturation pressure for water

Temp. (°C)	Pa	Temp. (°C)	Pa
0	608	50	12 330
10	1226	60	19 920
20	2334	70	31 160
30	4236	80	47 360
40	7375	100	101 320

Table 9.4 Solubility of air in water

Temp. (°C)	0	20	40	60	80	100
Air	0.028 8	0.018 7	0.014 2	0.012 2	0.011 3	0.011 1

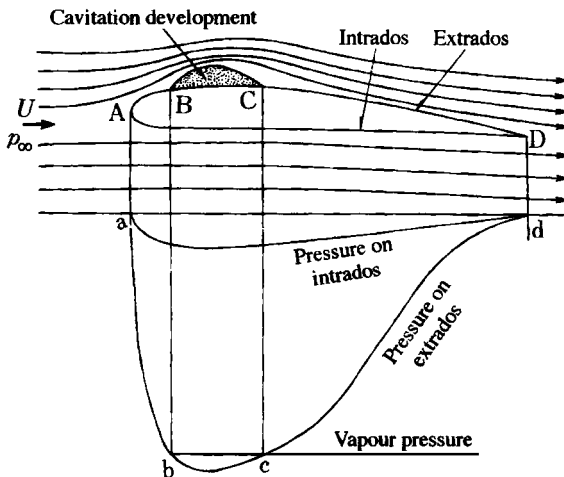


Fig. 9.25 Development of cavitation on an aerofoil section

$$k_d = \frac{p_\infty - p_v}{\rho U^2 / 2} \quad (9.35)$$

k_d in this equation is called the cavitation number. When k_d is small, cavitation is likely to develop.

9.6 Problems

1. Obtain the terminal velocity of a spherical sand particle dropping freely in water.

2. A wind of velocity 40 m/s is blowing against an electricity pole 50 cm in diameter and 5 m high. Obtain the drag and the maximum bending moment acting on the pole. Assume that the drag coefficient is 0.6 and the air density is 1205 kg/m^3 .
3. A smooth spherical body of diameter 12 cm is travelling at a velocity of 30 m/s in windless open air under the conditions of 20°C temperature and standard atmospheric pressure. Obtain the drag of the sphere.
4. If air at standard atmospheric pressure is flowing at velocity of 4 km/h along a flat plate of length 2.5 m, what is the maximum value of the boundary layer thickness? What is it when the wind velocity is 120 km/h?
5. What are the torque and the power necessary to turn a rotor as shown in Fig. 9.13 at 600 rpm in oil of specific gravity 0.9? Assume that the friction coefficient $f = 0.147$, $r_0 = 30 \text{ cm}$ and $b = 5 \text{ cm}$.
6. When walking on a country road in a cold wintry wind, whistling sounds can be heard from power lines blown by the wind. Explain the phenomenon by which such sounds develop.
7. In a baseball game, when the pitcher throws a drop or a curve, the ball significantly and suddenly goes down or curves. Find out why.
8. An oblong barge of length 10 m, width 2.5 m and draft 0.25 m is going up a river at a relative velocity of 1.5 m/s to the water flow. What are the friction resistance suffered by the barge and the power necessary for navigation, assuming a water temperature of 20°C ?
9. If a cylinder of radius $r = 3 \text{ cm}$ and length $l = 50 \text{ cm}$ is rotating at $n = 1000 \text{ rpm}$ in air where a wind velocity $u = 10 \text{ m/s}$, how much lift is produced on the cylinder? Assume that $\rho = 1.205 \text{ kg/m}^3$ and that air on the cylinder surface does not separate.
10. A car of frontal projection area 2 m^2 is running at 60 km/h in calm air of temperature 20°C and standard atmospheric pressure. What is the drag on the car? Assume that the resistance coefficient is 0.4.